

Vertical density waves in the Milky Way disc induced by the Sagittarius Dwarf Galaxy

Facundo A. Gómez^{1,2*}, Ivan Minchev³, Brian W. O’Shea^{1,2,4,5}, Timothy C. Beers^{6,1,5}, James S. Bullock⁷, Chris W. Purcell⁸

¹ Department of Physics and Astronomy, Michigan State University, East Lansing, MI 48824, USA

² Institute for Cyber-Enabled Research, Michigan State University, East Lansing, MI 48824, USA

³ Leibniz-Institut für Astrophysik Potsdam (AIP), An der Sternwarte 16, D-14482, Potsdam, Germany

⁴ Lyman Briggs College, Michigan State University, East Lansing, MI 48825, USA

⁵ Joint Institute for Nuclear Astrophysics (JINA), Michigan State University, East Lansing, MI 48824, USA

⁶ National Optical Astronomy Observatory, Tucson, AZ 85719, USA

⁷ Department of Physics & Astronomy 4129 Frederick Reines Hall, University of California, Irvine, CA 92697, USA

⁸ Department of Physics and Astronomy, University of Pittsburgh, Pittsburgh, PA 15260, USA

ABSTRACT

Recently, Widrow and collaborators announced the discovery of vertical density waves in the Milky Way disk. Here we investigate a scenario where these waves were induced by the Sagittarius dwarf galaxy as it plunged through the Galaxy. Using numerical simulations, we find that the the Sagittarius impact produces North-South asymmetries and vertical wave-like behavior that qualitatively agrees with what is observed. The extent to which vertical modes can radially penetrate into the disc, as well as their amplitudes, depend on the mass of the perturbing satellite. We show that the mean height of the disc is expected to vary more rapidly in the radial than in the azimuthal direction. If the observed vertical density asymmetry is indeed caused by vertical oscillations, we predict radial and azimuthal variations of the mean vertical velocity, correlating with the spatial structure. These variations can have amplitudes as large as 8 km s^{-1} .

Key words: Galaxy: disc, structure – galaxies: formation – galaxies: kinematics and dynamics – methods: N -body simulations

1 INTRODUCTION

Minor mergers can significantly perturb the overall structure of their host galactic disc (Quinn et al. 1993; Villalobos & Helmi 2008). As they merge, relatively small satellite galaxies can induce the formation of spiral arms and ring-like structures as well as radial migration, significantly flare or warp the disc, and influence the growth of a central bar (Tutukov & Fedorova 2006; Kazantzidis et al. 2008; Villalobos & Helmi 2008; Younger et al. 2008; Minchev et al. 2009; Quillen et al. 2009; Purcell et al. 2011; Bird et al. 2012; Gómez et al. 2012b).

Purcell et al. (2011, hereafter P11) presented simulations of the response of the Milky Way (MW) disc to tidal interaction with the Sagittarius dwarf galaxy (Sgr). They showed that many of the global morphological features ob-

served in the Galactic disc can be simultaneously explained by this interaction. An example is the kinematically cold structure known as the Monoceros ring (Newberg et al. 2002; Jurić et al. 2008), which naturally emerges in these simulations, although its origin is still a matter of debate (see Conn et al. 2012; Li et al. 2012; Lopez-Corrodoira et al. 2012). Gómez et al. (2012a, hereafter G12) showed that perturbations observed in the phase-space distribution of old disc stars in the Solar Neighbourhood (SN) can be reproduced qualitatively with these simulations. They interpreted such perturbations as signatures of *radial* density waves excited on the plane of the disc by Sgr. Perturbations in the *vertical* direction were not explored in their work. However, using a much larger photometric and spectroscopic data set, Widrow et al. (2012, hereafter W12) recently identified a North-South asymmetry in both the spatial density and the velocity distribution of SN stars. The asymmetry has the appearance of a coherent, wave-like perturbation, intrinsic to

* Email:fgomez@pa.msu.edu

the disc. W12 speculate that this perturbation could have been excited by the passage of a satellite galaxy through the Galactic disc. In this Letter, we explore the possibility of Sgr being the perturber associated with *both* the vertical and radial modes.

2 SIMULATIONS

In this Section we briefly describe our simulations; we refer the reader to P11 and G12 for a more detailed description. Two simulations with different models for the Sagittarius dwarf galaxy progenitor were performed. A Light (Heavy) *Sgr* progenitor, with effective virial mass $M_{\text{vir}} = 10^{10.5} M_{\odot}$ ($10^{11} M_{\odot}$), was initialised with a NFW dark matter halo of scale length 4.9 kpc (6.5 kpc), self-consistently with a separate stellar component. For the stellar component, a King profile with core radius 1.5 kpc, tidal radius 4 kpc, and a central velocity dispersion of 23 km s^{-1} (30 km s^{-1}) was used. The satellites were launched 80 kpc from the Galactic centre in the plane of the MW, traveling vertically at 80 km s^{-1} toward the North Galactic Pole. The mass loss that would have occurred between virial radius infall and this “initial” location is accounted for by truncating the progenitor DM halo mass profile at the instantaneous Jacobi tidal radius, $r_t = 23.2$ (30.6) kpc. This leaves a total bound mass that is a factor of ~ 3 smaller than the effective virial mass originally assigned. The simulations reach a present-day configuration after ≈ 2.7 Gyr (2.1 Gyr) of evolution. In both cases, the host galaxy includes a NFW dark matter halo with a scale radius $r_s = 14.4$ kpc and virial mass $M_{\text{vir}} = 10^{12} M_{\odot}$; the disc has a mass of $3.59 \times 10^{10} M_{\odot}$, an exponential scale length of 2.84 kpc, and a vertical scale height of 0.43 kpc; the central bulge has a mass of $9.52 \times 10^9 M_{\odot}$ and an $n = 1.28$ Sérsic profile, with an effective radius of 0.56 kpc. The initial disc in both *Sgr*-infall models is completely smooth at $t = 0$ Gyr. The simulations followed the evolution of 30 million particles with masses in the range $1.1 - 1.9 \times 10^4 M_{\odot}$.

3 PERTURBATIONS IN LOCAL VOLUMES

Fig. 1 shows an overdensity map of the Heavy (left) and Light (right) *Sgr* simulation discs at present-day configuration. The maps are obtained by normalising the local stellar density to the mean axisymmetric density at the corresponding galactocentric distance. The non-axisymmetric energy kick imparted by the satellite as it merges with the host induces the formation of spiral density waves. As shown by G12, waves excited by the Heavy *Sgr* satellite can be detected in SN-like volumes as peaks in the local energy distribution. These density waves are mainly in the radial direction. In fact, in very small local volumes (i.e., distances ≤ 0.2 kpc), these waves can be observed as well-defined features in the radial (v_r) and tangential (v_{ϕ}) velocity field (see Minchev et al. 2009, G12). In the left panel of Fig. 2, we show with dashed lines the normalised total energy distribution $E = f(\mathbf{x}, \mathbf{v})$ of two SN-like cylindrical volumes extracted from the Heavy *Sgr* simulation. The volumes have a 1 kpc radius, and are located at 8 kpc from the galactic centre. Their locations, chosen based on G12 results, are indicated

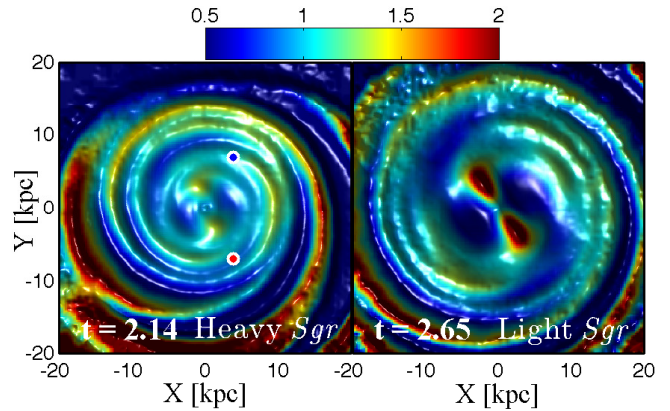


Figure 1. Overdensity map of the Heavy (left) and Light (right) *Sgr* simulations at the present time. The colours and relief indicate the ratio of the local stellar density to the mean axisymmetric disc density at the corresponding galactocentric distance. The blue and red dots indicate the location of the volumes explored.

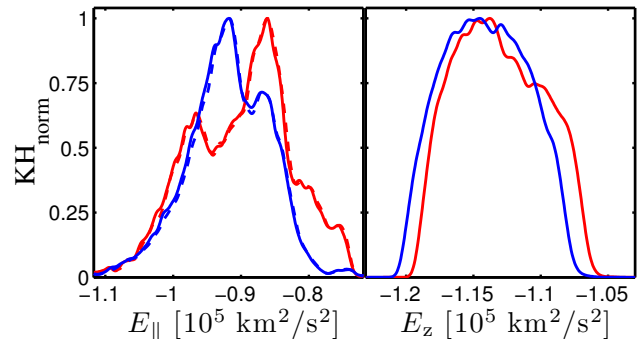


Figure 2. *Left panel:* Total (dashed lines) and in-plane (solid lines) energy distributions of disc particles located within the blue and red volumes shown in Fig. 1. *Right panel:* As in the left panel, but for the vertical energy distribution.

with a blue and a red dot in the left panel of Fig. 1. Note the well-defined peaks in these distributions, which reveal the presence of density waves. As expected from disc orbits, the in-plane energy distribution $E_{\parallel} = f(\mathbf{x}, v_r, v_{\phi})$ (solid lines) is very similar to the total energy distribution, indicating that these peaks are associated with perturbations mainly in the plane of the disc. Nevertheless, the stellar particles in these volumes present non-symmetrical energy distributions in the vertical direction $E_z = f(\mathbf{x}, v_z)$, as shown in the right panel of Fig. 2. Furthermore, these distributions are shifted with respect to one another.

To explore whether the asymmetries and shifts observed in the E_z distributions are indications of *vertical* density waves, we compute for both volumes the distribution of stellar particles as a function of height with respect to the midplane of the galactic disc, $n(Z)_{|R,\theta}$, or simply $n(Z)$. A north-south asymmetry in this distribution could be an indication of vertical modes (see W12). To compute $n(Z)$, we have carefully aligned the disc with the X-Y plane. This is done by iteratively computing, and aligning with the Z-direction, the total angular momentum of the disc particles located within 4 kpc radius cylinders of decreasing height. In order to identify signatures of vertical density waves, it is desirable to compare $n(Z)$ obtained from the perturbed disc

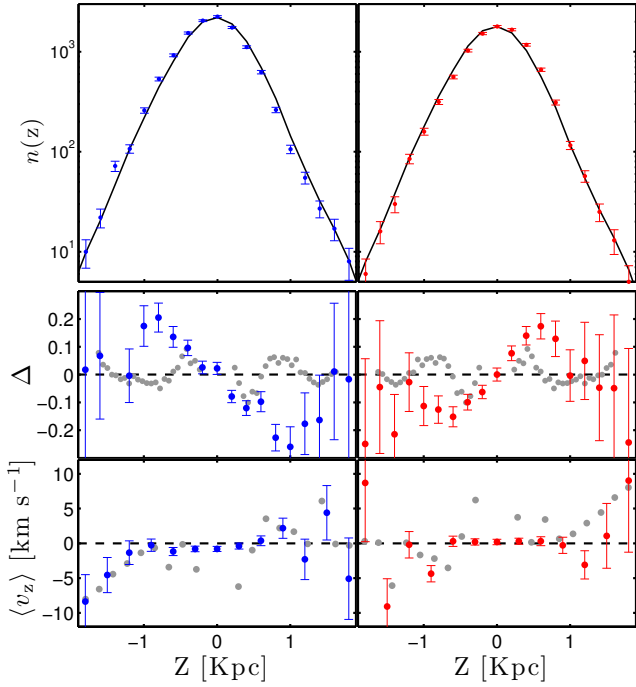


Figure 3. *First row:* The blue and red dots show the distribution of particles as a function of height, $n(Z)$, with respect to the midplane of the disc, obtained from the volumes shown in Fig. 1. The black solid lines show a model of the underlying smooth distribution $n_{\text{av}}(Z)$. *Second row:* Distribution of the residuals, $\Delta = (n(Z) - n_{\text{av}}(Z))/n_{\text{av}}(Z)$, for both volumes. *Third row:* Mean vertical velocity as a function Z . Error bars indicate Poisson noise. The grey dots show observational data from W12. On the right-hand panels we have shifted the observational data with respect to the axes $Z = 0$ and $v_z = 0$ to match the phases of the waves.

with its corresponding smooth underlying distribution. For this purpose, W12 fitted a smooth two-component model to their stellar sample’s number density. In this work we follow a different approach: we obtain a *smooth* distribution of stellar particles, as a function of height, by azimuthally averaging $n(Z)$ i.e.,

$$n_{\text{av}}(Z)|_R = (2\pi)^{-1} \int_0^{2\pi} n(Z, \theta)|_R d\theta.$$

Our assumption is that local asymmetries of this distribution are erased after averaging over all azimuthal angles. In addition, we expect $n_{\text{av}}(Z)|_R$ to be a better representation of the true smooth height distribution of particles than smooth analytic fits. The top panels of Fig. 3 show, with coloured dots, the $n(Z)$ distributions obtained from the “blue” and “red” volumes in Fig. 1, whereas the black solid line corresponds to $n_{\text{av}}(Z)$. Note that $n_{\text{av}}(Z)$ was re-normalised to the total number of particle in each volume. Due to finite particle numbers, we are able to reliably track $n(Z)$ only up to $|Z| \approx 1.4$ kpc. These panels indicates a shift of the local with respect to the smooth distribution, although this occurs in different directions for the two cases. Note, however, that for large $|Z|$ (i.e. $\gtrsim 0.7$ kpc), the shift in both distributions becomes progressively smaller, exhibiting a wave-like pattern. As in W12, we plot the residual,

$$\Delta = \frac{n(Z) - n_{\text{av}}(Z)}{n_{\text{av}}(Z)},$$

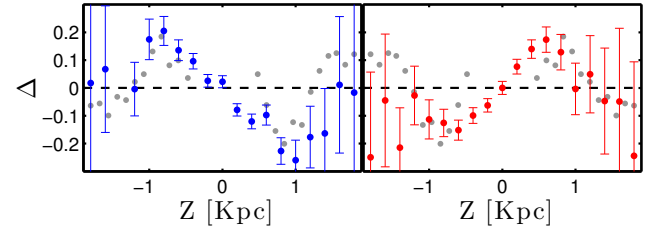


Figure 4. As in Fig. 4, after rescaling the amplitude and extent of the observed Δ by a factor of 2. On the right-hand panel we have shifted the observational data with respect to the axis $Z = 0$ to match the phases of the waves. Note the very similar wave-like behavior seen in the simulated and observed data sets.

to highlight these asymmetries. This is shown in the second row of Fig. 3 with blue and red dots. In both cases, Δ is an odd function of Z . The grey dots show data from Figure 1 of W12, derived from a sample of main-sequence stars in SDSS-DR8, the Eighth Data Release of the Sloan Digital Sky Survey (Aihara et al. 2011). To match the phases of the waves, on the right-hand panels we have shifted the observational data with respect to the axis $Z = 0$. At least within $|Z| < 1.4$ kpc, the residuals associated with our volumes present a similar wave-like behavior to that observed in the SN. However, the amplitude and extent of the perturbations found in this simulation are larger by a factor of ~ 2 . This indicates that either the Heavy Sgr model is too massive or that we are looking at the perturbation at an earlier stage. In addition, the lack of a gaseous disc component in these simulations is likely to play a significant role. A fraction of the energy imparted by the satellite should be absorbed by the gas, thus weakening the perturbation. In Fig. 4, we compare the observed and simulated Δ , after rescaling the observational data by the aforementioned factor. Note the very similar behavior of Δ observed in these two data sets. In the bottom row of Fig. 3, we show $\langle v_z \rangle$ as a function of Z . We note that results associated with this distribution should be taken with caution, due to their relatively low statistical significance. As before, grey dots indicate data extracted from the top panel of Figure 4 in W12. At large Z (≈ 1 kpc), the “blue” (“red”) volume shows a global trend towards negative (positive) values as Z decreases (increases). As explained by W12, this suggests a coherent motion of stellar particles away from the disc midplane.

It is important to realise that the phase-space distribution of the blue SN-like volume qualitatively reproduces not only the observed vertical structure (W12), as we just demonstrated, but also features seen in the plane of the local Galactic disk: As shown by G12, local samples of old disc stars present a total energy distribution that is in good agreement with the distribution shown in the left panel of Fig. 2 (blue lines).

4 AZIMUTHAL AND RADIAL DEPENDANCE

We have shown that the phase-space distributions of Solar Neighbourhood-like volumes extracted from our Heavy Sgr simulation exhibit wave-like perturbations in the vertical direction. However, it is not clear from the analysis shown thus far whether these are localised perturbations or are signatures of a global mode perturbing the entire disc.

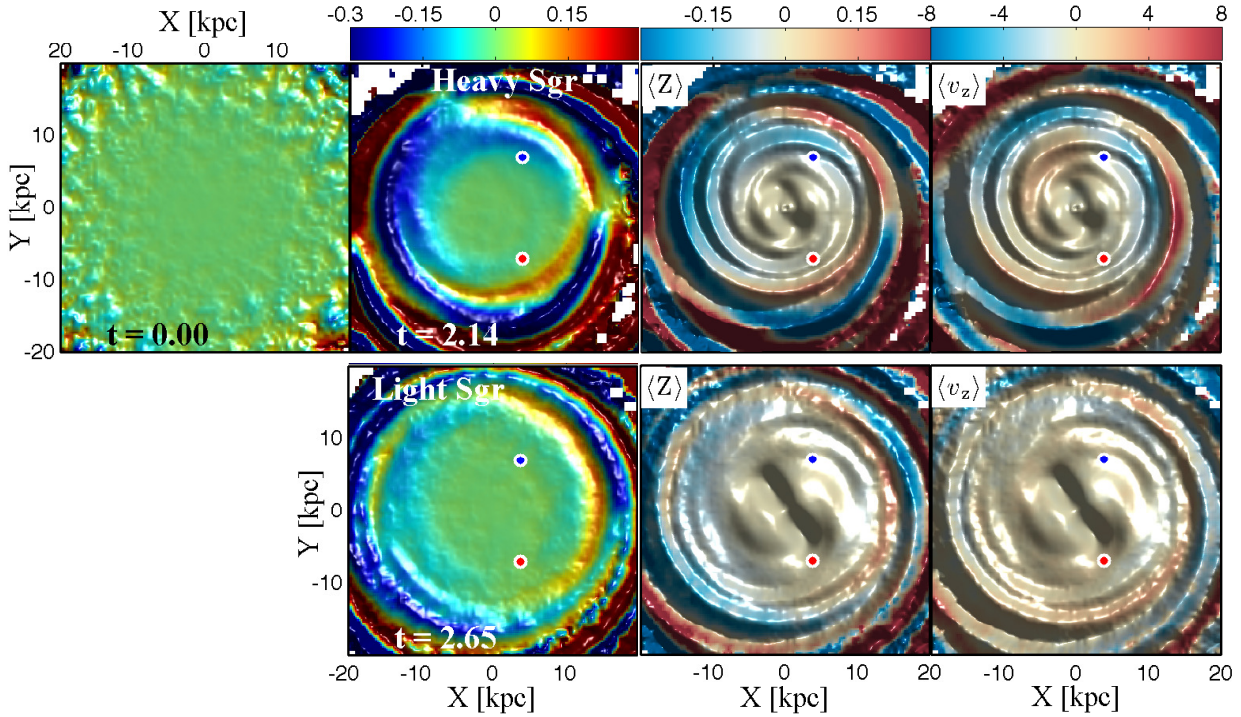


Figure 5. *First column:* Map of the simulated galactic disc’s mean height, $\langle Z \rangle$, at $t = 0$ Gyr, used in both simulations out to $R = 20$ kpc. *Second column:* Maps of the simulated galactic disc’s $\langle Z \rangle$ at present-day configuration, obtained from the Heavy (top) and Light (bottom) *Sgr* simulations, respectively. The different colours and relief indicate different values of $\langle Z \rangle$ in kpc. *Third column:* Different colours indicate different values of $\langle Z \rangle$ in kpc, whereas the relief traces the overdensity maps shown in Fig. 1. *Fourth column:* As before, but for the mean vertical velocity (in km s^{-1}). The coloured dots in the top panel indicate the location of the volumes analysed in Sec. 3.

From Fig. 3, we know that the $n(Z)$ distributions of the two analysed volumes are shifted with respect to one another, as well as with respect to $n_{\text{av}}(Z)$. If the observed shifts are signatures of vertical waves, we would expect to find correlations in the mean height of the disc $\langle Z \rangle$ as a function of galactocentric radius and azimuthal angle. We explore this in Fig. 5, where we show maps of $\langle Z \rangle$ for the Heavy and Light *Sgr* simulation disc out to $R \approx 20$ kpc. To obtain these maps, we grid the disc with a regular Cartesian mesh of bin size = 0.5 kpc aligned with the X-Y plane. On each grid node we centre a 1 kpc radius cylinder and compute $\langle Z \rangle$ by fitting a Gaussian distribution to $n(Z)$. In the top left panel, we show the $\langle Z \rangle$ -map reflecting the initial conditions of both discs at $t = 0$ Gyr. As expected from an initially unperturbed disc, the maps are consistent with $\langle Z \rangle = 0$ at all radii, except for small-scale departures due to finite particle resolution. The situation dramatically changes when we explore the present-day configurations. The second column of panels in Fig. 5 shows the $\langle Z \rangle$ -map of the Heavy (top) and Light (bottom) *Sgr* simulation’s discs, obtained after $t \approx 2.1$ and 2.6 Gyr, respectively. The colour coding indicates different values of $\langle Z \rangle$ and white regions represent volumes devoid of particles. We can now clearly identify wave-like, spiral perturbations traveling across the disc. It is possible to appreciate how the mean height of the disc gradually increases (decreases) as we follow one of these patterns azimuthally. Departures of $\langle Z \rangle$ with respect to the midplane can be as large as 0.3 kpc, especially for the Heavy *Sgr* simulation (top panels). The local volumes analysed previously are indicated with coloured dots. As expected from Fig. 3,

the blue (red) volume is located in a region lying slightly below (above) the midplane. In this simulation, the inner 7 kpc of the disc has not been strongly vertically perturbed by the satellite galaxy. Although the Light *Sgr* simulation (bottom panels) also exhibits wave-like perturbations, they generally have smaller amplitudes. Note that strong perturbations are observed only at $R \gtrsim 10$ kpc. In both cases, such boundary is located near corotation, where density waves are reflected backwards to the outer disc. This can be more clearly appreciated in panels A and B of Fig. 6, where we show the $\langle Z \rangle$ -maps in polar coordinates. The black dashed lines, at $R = 8$ kpc and $\theta = 1.06$ rad (measured with respect to the positive X semi-axis), cross at the location of the blue volume. For comparison, this location is indicated in both discs. Notice that the inner regions of the Light *Sgr* disc presents a value of $\langle Z \rangle \approx 0$ for a larger radial extent. Panel C in Fig. 6 shows $\langle Z \rangle$, as a function of θ , at $R = 8$ kpc for both discs. Significant vertical perturbations at this galactocentric radius can be observed only in the Heavy *Sgr* simulation. A dependance of $\langle Z \rangle$ with azimuthal angle θ is present. Panel D shows $\langle Z \rangle$, as a function of R , at $\theta = 1.06$ rad. In both discs, a well-defined wave-like pattern can be observed, with an amplitude increasing as a function of R . Note that $\langle Z \rangle$ exhibits a stronger dependance with galactocentric radius than with azimuthal angle; a result that could be contrasted against currently available stellar samples. In the third column of Fig. 5, we explore the relationship between these vertical patterns and the radial modes shown in Fig. 1. Here, the different colours indicate different values of $\langle Z \rangle$, whereas the relief traces overdense regions. Overdense

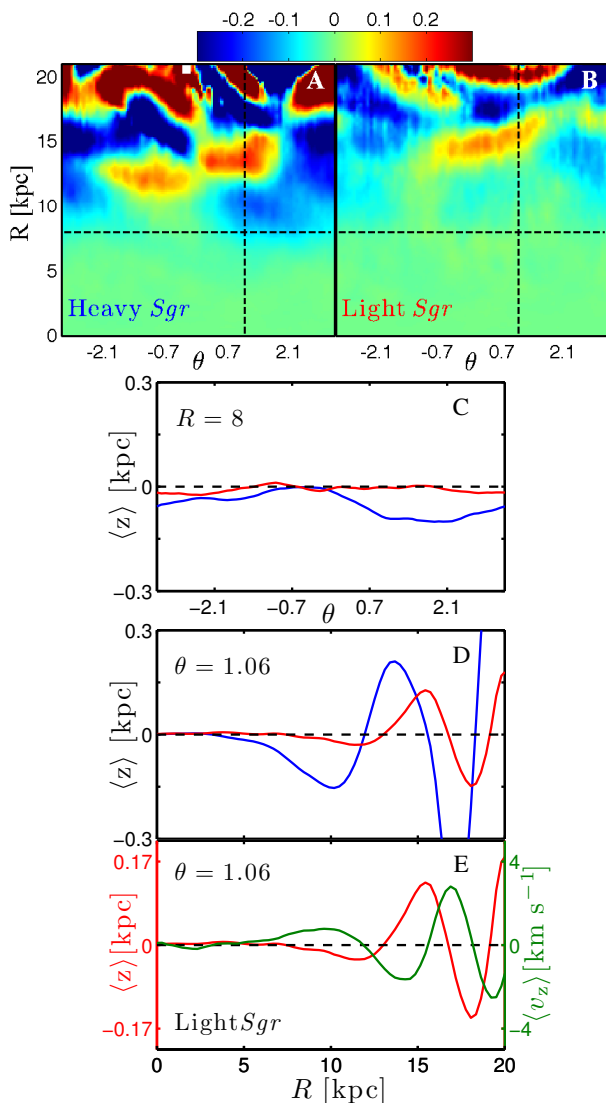


Figure 6. *Panels A and B:* Maps of the simulated galactic disc's, $\langle Z \rangle$, at present-day configuration obtained from the Heavy (left) and Light (right) *Sgr* simulations in polar coordinates (in kpc). The black dashed lines cross at the location of the blue volume shown in Fig 1. *Panels C and D* show the variation of the mean height of the disc as we move across the black dashed lines shown in the top panels. Blue and red lines are associated with the Heavy and Light *Sgr* simulation, respectively. *Panel E:* Comparison of the mean height (red) and vertical velocity (green), as a function of galactocentric radius obtained from the Light *Sgr* simulation.

features can be found both above and below the midplane. Furthermore, we can appreciate how the mean height of a given spiral arm changes as a function of the azimuthal angle.

If the observed patterns are indeed signatures of vertical density waves, a correlation between $\langle Z \rangle$ and the mean vertical velocity $\langle v_z \rangle$ is expected. We explore this in panel E of Fig. 6, where we plot, for the Light *Sgr* disc, $\langle Z \rangle$ and $\langle v_z \rangle$ as a function of R , at a fixed azimuthal angle. A wave-like pattern is also observed in $\langle v_z \rangle$. At galactocentric radii where $\langle Z \rangle$ takes an extrema, $\langle v_z \rangle \approx 0$. On the other hand, at galactocentric radii where $\langle v_z \rangle$ takes a maximum or a minimum value, $\langle Z \rangle \approx 0$. This is exactly what is expected from oscil-

latory behaviour. In the last column of Fig. 5 we show, with different colours, the local $\langle v_z \rangle$ for both galactic disc. The relief in these panels traces the corresponding overdensity maps. Note again the wave-like structure of these patterns. In the Heavy *Sgr* simulation (top panel), $\langle v_z \rangle$ can depart from 0 km s^{-1} by more than 8 km s^{-1} . Similarly to what is observed for $\langle Z \rangle$, the $\langle v_z \rangle$ of a given spiral arm varies as a function of the azimuthal angle, changing from positive to negative departures with respect to $\langle v_z \rangle = 0 \text{ km s}^{-1}$.

5 THE MAGELLANIC CLOUDS AS OTHER POSSIBLE CULPRIT

We have focused our attention on perturbations induced by the *Sgr* dwarf galaxy. However, the Large Magellanic Cloud (LMC) have been considered in the past by several authors as a plausible perturber behind the warp observed in the MW disk's H I layer (Kalberla & Kerp 2009). Given its traditional mass ($\sim 2\%$ of the MW mass) and location ($\sim 50 \text{ kpc}$) estimates, the LMC tidal field is not sufficiently strong to induce the observed vertical perturbation (e.g. Hunter & Toomre 1969; Besla et al. 2007, hereafter B07). Nonetheless, the addition of the force from the dark matter halo wake excited by the Clouds (Weinberg 1998) could be enough to account for the observed warp (Weinberg & Blitz 2006). The previous results, based on linear perturbation theory, were tested with fully self-consistent simulations by Tsuchiya (2002). Assuming a decaying orbit for the LMC, this analysis showed that the observed warp could be reproduced over a 6 Gyr timescale, involving approximately four full orbital periods (see also García-Ruiz et al. 2002, for a different opinion). This orbital configuration is at odds with the recent findings by B07, which suggested that the Magellanic Clouds are approaching the MW for the very first time on a parabolic orbit traveling at $\sim 400 \text{ km/s}$. However, Vesperini & Weinberg (2000) showed that the perturbation excited by a low-velocity ($\sim 200 \text{ km/s}$) flyby encounter with a slightly more massive satellite ($> 5\%$ of the MW mass) can be efficiently transmitted to the inner regions of the dark matter halo, where it can affect the structure of an embedded stellar disk. More recent estimates of the total LMC mass, based on abundance matching techniques, suggested values as large as 10% of the MW mass (Boylan-Kolchin et al. 2011). Moreover, the orbits of the MCs are currently being revised (Kallivayalil et al., in preparation). New dynamical models, including both updated orbital parameters and total mass estimates, are required to assess whether such a mechanism would have sufficient time to operate. We defer this analysis to future work.

6 DISCUSSION

In this work, we have explored a scenario in which *Sgr* is the perturber behind the North-South asymmetry recently observed in the number density and mean vertical velocity of Solar Neighbourhood stars (W12). For this purpose, we have searched for both local and global signatures of vertical density waves in two simulations modelling the response of the MW to the infall of *Sgr*. Distributions of stellar particles as a function of height in Solar Neighbourhood-like volumes

extracted from our more massive Sgr's progenitor simulation present clear indications of a perturbation in the vertical direction of the disc. This asymmetry becomes more evident when comparing to a model of the underlying smooth vertical distribution of particles. Within the $|Z|$ -range allowed by our finite mass resolution, the phase-space distribution of certain SN-like volumes can qualitatively reproduce the North-South asymmetry observed by W12. Remarkably, the same phase-space distributions can simultaneously reproduce the signatures of radial density waves observed by G12.

By creating maps of the mean height of the disc within $R \leq 20$ kpc, we have shown that the vertical perturbations observed in local volumes are signatures of a global mode perturbing the entire disc. As in the case of the radial density modes (G12), the amplitude and the extent to which vertical modes can radially penetrate into the disc depends on the mass of the perturbing satellite. Interestingly, we have shown that the mean height of the disc is expected to vary much more rapidly in the radial than in the azimuthal direction. Furthermore, the mean height of overdense spiral features vary azimuthally, moving from below to above the midplane of the disc. Signatures of vertical modes should also be observable in maps of the Galactic disc's mean vertical velocity since, not surprisingly, they present a clear oscillatory behavior.

In contrast to radial modes that can be excited by a number of different external and internal mechanisms, vertical modes *must be excited* by some agent external to the disc. Although we have shown that perturbations induced by Sgr could be enough to account for several features observed in the Solar Neighborhood, it is likely that MCs are playing a role in shaping the vertical structure of MW disc. We plan to characterize the coupling of these two perturbations in a follow-up study. Contrasting the results presented in this work against currently available samples of Galactic disc stars could help to understand the origin of the observed vertical and in-plane perturbations.

ACKNOWLEDGMENTS

We would like to thank the anonymous referee for the useful comments and suggestions which helped to improve this paper. The authors wish to thank Gurtina Besla for insightful discussions. FAG was supported through the NSF Office of Cyberinfrastructure by grant PHY-0941373, and by the Michigan State University Institute for Cyber-Enabled Research. BWO was supported in part by the Department of Energy through the Los Alamos National Laboratory Institute for Geophysics and Planetary Physics. TCB acknowledges partial support from grant PHY 08-22648: Physics Frontiers Center/Joint Institute for Nuclear Astrophysics (JINA), awarded by the U.S. National Science Foundation.

REFERENCES

- Aihara H. et al., 2011, ApJ, 193, 29
 Besla G., Kallivayalil N., Hernquist L., Robertson B., Cox T. J., van der Marel R. P., Alcock C., 2007, ApJ, 668, 949
 Bird J. C., Kazantzidis S., Weinberg D. H., 2012, MNRAS, 420, 913
 Boylan-Kolchin M., Besla G., Hernquist L., 2011, MNRAS, 414, 1560
 Conn B. C. et al., 2012, ApJ, 754, 101
 García-Ruiz I., Kuijken K., Dubinski J., 2002, MNRAS, 337, 459
 Gómez F. A. et al., 2012a, MNRAS, 423, 3727
 Gómez F. A., Minchev I., Villalobos Á., O'Shea B. W., Williams M. E. K., 2012b, MNRAS, 419, 2163
 Hunter C., Toomre A., 1969, ApJ, 155, 747
 Jurić M. et al., 2008, ApJ, 673, 864
 Kalberla P. M. W., Kerp J., 2009, ARA&A, 47, 27
 Kazantzidis S., Bullock J. S., Zentner A. R., Kravtsov A. V., Moustakas L. A., 2008, ApJ, 688, 254
 Li J., Newberg H. J., Carlin J. L., Deng L., Newby M., Willett B. A., Xu Y., Luo Z., 2012, ApJ, 757, 151
 Lopez-Corrodoira M., Moitinho A., Zaggia S., Momany Y., Carraro G., Hammersley P. L., Cabrera-Lavers A., Vazquez R. A., 2012
 Minchev I., Quillen A. C., Williams M., Freeman K. C., Nordhaus J., Siebert A., Bienaymé O., 2009, MNRAS, 396, L56
 Newberg H. J. et al., 2002, ApJ, 569, 245
 Purcell C. W., Bullock J. S., Tollerud E. J., Rocha M., Chakrabarti S., 2011, Nature, 477, 301
 Quillen A. C., Minchev I., Bland-Hawthorn J., Haywood M., 2009, MNRAS, 397, 1599
 Quinn P. J., Hernquist L., Fullagar D. P., 1993, ApJ, 403, 74
 Tsuchiya T., 2002, NewA, 7, 293
 Tutukov A. V., Fedorova A. V., 2006, Astronomy Reports, 50, 785
 Vesperini E., Weinberg M. D., 2000, ApJ, 534, 598
 Villalobos Á., Helmi A., 2008, MNRAS, 391, 1806
 Weinberg M. D., 1998, MNRAS, 299, 499
 Weinberg M. D., Blitz L., 2006, ApJ, 641, L33
 Widrow L. M., Gardner S., Yanny B., Dodelson S., Chen H.-Y., 2012, ApJ, 750, L41
 Younger J. D., Besla G., Cox T. J., Hernquist L., Robertson B., Willman B., 2008, ApJ, 676, L21